American Mineralogist, Volume 58, pages 243-248, 1973

Combined Electron Microscopy and Analysis of an Orthopyroxene

G. W. LORIMER
Department of Metallurgy, Faculty of Science, University of Manchester, Manchester M13 9PL, England

P. E. CHAMPNESS
Department of Geology, Faculty of Science, University of Manchester, Manchester M13 9PL, England

Abstract

A bronzite containing exsolved augite has been examined by combined transmission electron microscopy and microprobe analysis in the analytical electron microscope, EMMA-4. Heterogeneously-distributed augite lamellae up to 0.5μ thick were observed parallel to (100) of the matrix.

EMMA-4 has been used to measure the solute concentration-profile adjacent to the lamellae and to estimate their composition. The analyses indicate that the lamellae are augite containing approximately 24 wt percent CaO.

Introduction

The orthopyroxene is a bronzite with composition approximately $Mg_{.81}Fe_{.16}Ca_{.03}Si_2O_6$ from the Stillwater Complex, Montana (Hess, 1960) which exhibits a lamellar structure parallel to (100) under the polarizing microscope. Such structures are common in orthopyroxenes of plutonic rocks. In a study of their origin by Henry (1942), single crystal X-ray studies of several specimens failed to prove the existence of a second phase but showed a second set of reflections joined to the first by Debye-Scherrer curves. Henry concluded that the lamellae had the same composition as the matrix and were formed by deformation.

Hess (1960) took X-ray single crystal photographs of the Stillwater bronzites and confirmed Henry's experimental results, but found that the disorientation could be seen optically and was entirely in the orthopyroxene host. He concluded that, because the lamellae had a higher birefringence than the matrix, they were exsolved augite but that their volume fraction was too small to produce reflections on single crystal X-ray photographs.

Recently Boyd and Brown (1969) examined a bronzite from the Stillwater Complex in an electron probe microanalyzer. The CaKα scan showed a variation which they attributed to the exsolution of a calcium-rich phase in the orthorhombic host, but the resolution of the instrument was not sufficient to enable quantitative analysis of either the matrix or the exsolved phase. Boyd and Brown estimated that the lamellae were 1 to 2μ thick and suggested that the volume fraction of lamellae was too large for them to have an augite composition.

Champness and Lorimer (1973) examined the same bronzite in the transmission electron microscope. They found that the lamellae were exsolved clinopyroxene up to 0.5μ thick and were semi-coherent with the matrix. Examination of the distribution of the phases in the high-voltage electron microscope showed that the exsolved phase comprises only about 1.4 percent by volume. Figure 1 is a general view of the microstructure in which the lamellae are approximately parallel to the electron beam. Between the large lamellae there is a fine distribution of coherent G.P. (Guinier-Preston) zones. A precipitate-free zone (PFZ) occurs adjacent to each clinopyroxene lamellae. It was the purpose of this investigation to use the analytical electron microscope, EMMA-4, to examine the Ca-distribution between the lamellae and to estimate the composition of the clinopyroxene.

The Analytical Electron Microscope Emma-4

EMMA-4 has been designed as a combined high resolution electron microscope and microprobe analyzer.[1] The instrument can be operated at accel-

[1] EMMA-4 is manufactured by AEI Scientific Apparatus Division and has been developed in conjunction with Dr. P. Duncumb, Dr. C. J. Cooke, and the staff of Tube Investment Research Laboratories (Cooke and Duncumb, 1968).

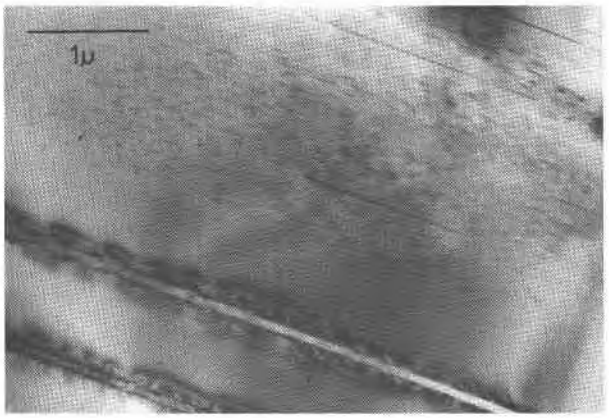

FIG. 1. Electron micrograph of the bronzite taken at 100 kV, showing large lamellae parallel to (100) matrix, a fine distribution of coherent G.P. zones, thin lamellae parallel to (100) matrix and PFZS (precipitate free zones) adjacent to both the thick and thin lamellae.

erating voltages of 40, 60, 80 and 100 kV and has a spatial resolution of approximately 7 Å at 100 kV. When the instrument is used in its analytical mode, the second condenser lens is switched off and the mini lens, an extra lens situated between the second condenser and the specimen, is activated to form a highly convergent beam at the specimen (Fig. 2). With a circular beam it is possible to obtain a probe size of less than 0.2μ and a probe current of 10 to 20 nA. X-rays produced in the specimen can be detected with either a nondispersive detector or two linear fully-focusing spectrometers; both facilities have an X-ray take-off angle of 45° and employ gas-flow proportional counters.

The obvious forté of the instrument is that it enables correlation of petrographic detail and diffraction data observed in the electron microscope with chemical composition. The probe diameter at the specimen of 0.1-0.2μ is approximately 4 to 5 times smaller than that obtainable in conventional microprobe analyzers. Also, because the specimen must be thin enough for transmission electron microscopy at 100 kV—that is, about 0.2μ for silicate minerals—very little diffusion of the electron beam occurs within the sample; the bell-shaped region beneath the surface of a bulk specimen from which the majority of X-rays originate during conventional microprobe analysis is absent. This results in a further two or three-fold decrease in effective probe size. Thus the true probe size of 0.1-0.2μ obtainable using EMMA-4 is at least an order of magnitude smaller than that in the conventional microprobe analyzer. A further decrease in the beam width to less than 0.05μ in one direction can be realized by purposely making the beam astigmatic.

Quantitative Analysis

Quantitative microprobe analysis of bulk specimens is based on the comparison of the characteristic X-ray intensity from an element in the specimen with the characteristic X-ray intensity from the same element in a suitable standard, followed by the application of various correction procedures to account for back scattering, X-ray absorption and fluorescence. In a specimen which is thin enough to be examined by transmission electron microscopy, the intensity of the characteristic X-rays produced cannot be compared with a bulk standard because the observed X-ray intensity is a function of foil thickness and the large variations in foil thickness, which typify specimens prepared by ion thinning, make it impractical to prepare thin-film standards.

However, in a specimen which is sufficiently 'thin' so that the primary X-rays produced by the incident beam have a low probability of either being absorbed or of exciting fluorescent radiation in the sample, a simple technique can be used to determine weight-fraction ratios (Lorimer *et al.*, 1972; Cliff and Lorimer, 1972). The ratio of the characteristic X-ray intensities from two elements I_1/I_2 is related to the weight fraction ratio C_1/C_2 by the simple expression

$$I_1/I_2 = k\, C_1/C_2$$

where k is a constant which includes the corrections for the efficiency of production and detection of

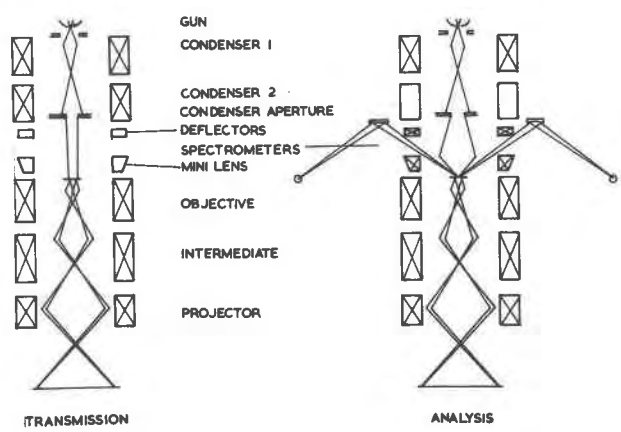

FIG. 2. Schematic ray diagram of the electron trajectories during the operation of EMMA-4 in the Microscopy and Analysis modes (from Lorimer *et al.*, 1972).

X-rays for the two elements. If the average composition of the sample is known and if the scale of chemical inhomogeneities is less than the scale of the area transparent to the electron beam, typically a few tens of microns, then the constant k can be determined by spreading the illumination so that it covers an area which is representative of the bulk composition and measuring I_1 and I_2. Alternatively k can be determined by measuring I_1 and I_2 in a thin specimen of known composition. Once k has been calculated, the beam can be focused into a small probe and local variations in weight fraction can be obtained by multiplying the observed characteristic ratio by $1/k$. The two X-ray intensities are measured simultaneously on the two spectrometers, and thus the observed X-ray intensity ratio is independent of variations in probe current.

For this simple technique of analysis to be valid, the sample must be thin enough so that the primary X-rays produced are not attenuated in the specimen. To determine this thin-foil limit for X-ray analysis, the intensity of the characteristic radiation from the element to be analyzed and the intensity of a band of the continuous X-ray spectrum are plotted as a function of specimen thickness. The intensity of the white radiation is taken as a measure of the specimen thickness (Hall, 1971), and the intensity of the characteristic radiation as a measure of the weight fraction of the element in question. The point at which there is a deviation from linearity in a plot of the characteristic radiation versus the white radiation is taken as the thin-foil limit for X-rays; *i.e.,* the specimen thickness at which corrections must be made for X-ray absorption and/or fluorescence.

A graph of the intensity of CaKα and of SiKα versus a band of the white radiation as a function of specimen thickness for an ion-thinned glass standard[2] is shown in Figure 3. The point at which the specimen becomes too thick to carry out conventional electron microscopy at 100 kV is indicated as the "transmission limit" on both the graphs. As can be seen from Figure 3, there is no significant deviation from a straight-line relationship; *i.e,* the specimen is 'thin' as far as X-ray analysis is concerned at a specimen thickness well in excess of that usually used for transmission electron microscopy.

[2] The glass standard was made by the single fusion of a gel produced by standard techniques and contained 65 mole percent diopside, 35 mole percent jadeite. The ratio of SiKα/CaKα was also constant for thicknesses up to and beyond the transmission limit.

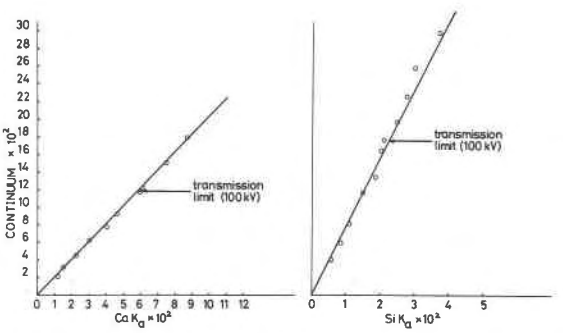

FIG. 3. Graph of intensity of CaKα and SiKα *vs* a portion of the continuous spectrum for various specimen thicknesses at 100 kV and a 4nA beam current. The thin-foil limit for conventional transmission electron-microscopy at 100 kV is marked.

A similar analysis has been carried out for a number of metal alloys (Lorimer *et al.,* 1972; Cliff and Lorimer, 1972), and it appears to be a general criterion that those regions of the specimen which are thin enough to carry out transmission electron microscopy are also transparent to the primary X-rays so that the simple ratio technique can be used to carry out quantitative analysis.

Analysis of the Clinopyroxene Lamellae

Samples for electron microscopy were prepared from conventional uncovered petrographic thin sections using the techniques described by Barber (1970) and Champness and Lorimer (1971) which enable a direct correlation to be made between the optical and electron optical microstructures. Each sample was thinned in an Edwards IBMA-1 ion-thinning machine until perforation occurred. Specimens were then examined in the analytical electron microscope.

The bronzite proved to be chemically inhomogeneous on too coarse a scale to serve as its own standard for quantitative analysis. Consequently, two external standards were used: one was an ion-thinned sample of the jadeite/diopside glass mentioned above and the second was an ion-thinned specimen of pigeonite from the Isle of Mull (Hallimond, 1914) which contained 3.80 wt percent CaO. A calcium scan in the conventional electron-probe microanalyzer had previously shown that the latter specimen was chemically homogeneous.

For the quantitative analysis of the clinopyroxene, the widest lamella in the specimen (about 0.5μ as shown in Figure 4) was chosen and the electron beam was focused to a diameter of approximately 0.2μ.

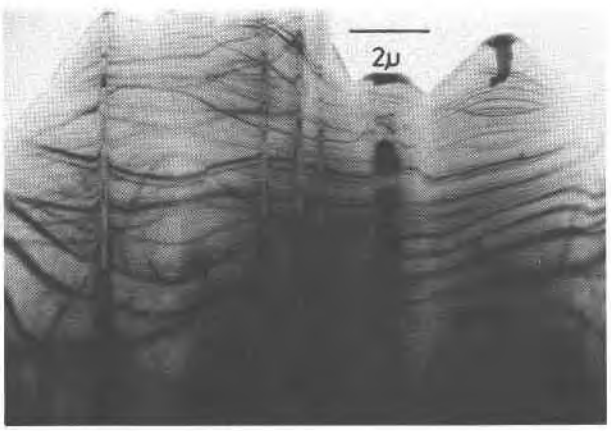

FIG. 4. Electron micrograph of a large lamella. The contamination spots mark the position of the electron probe during analysis.

The contamination spots (Fig. 4) mark the position of the beam during the analysis. The probe diameter, beam width at half peak-height, is approximately equal to the diameter of the inner ring of the contamination spot.[3]

The intensities of the calcium and silicon characteristic radiations were monitored simultaneously, one on each spectrometer. Before and after the analysis of the lamellae, the two standards were analyzed without making any adjustment to the position of the spectrometers. After the characteristic intensities had been monitored, the background radiations were determined for both elements on all three samples. The relevant data from these analyses are given in Table 1. The Ca/Si ratio was calculated for the clinopyroxene using the constant k determined from the measurements made on the two standards.

In Figure 5 the Ca/Si weight fraction has been plotted as a function of atomic percent iron for calcium-rich and calcium-poor co-existing phases in the Bushveld Complex (Atkins, 1969). The bulk composition of the Stillwater bronzite is shown at S, and the Ca/Si ratios measured for the exsolved clinopyroxene have been plotted along a tie-line parallel to those for co-existing Bushveld phases. It can be seen that the clinopyroxene is an augite, not a subcalcic augite as suggested by Boyd and Brown

TABLE 1. EMMA-4 Data for the Analysis of the Clinopyroxene

Sample	Total counts corrected for background			k	Weight ratio Ca/Si*
	Ca	Si	Ca/Si		
Clinopyroxene lamella	4039	1026	3.94 ± 0.18	-	-
Glass Standard	2735	985	2.78 ± 0.14	5.97 ± 0.30	0.66 ± 0.04
Mull Pigeonite Standard	975	1567	0.622 ± 0.036	5.33 ± 0.30	0.74 ± 0.05

* on sample using constant k

(1969) and that it is significantly richer in calcium than the augites in the Bushveld Complex.[4]

As the silicon content in the pyroxene quadrilateral is almost constant, it is possible to estimate the weight percent of calcium from the Ca/Si ratios in Table 1. Assuming that the SiO_2 content is about 53 wt percent, as estimated from analyses of augites of approximately the same composition from the Bushveld Complex given by Atkins (1969), the calcium content is 17.3 ± 0.2 wt percent Ca or 24.2 ± 0.2 wt percent CaO.

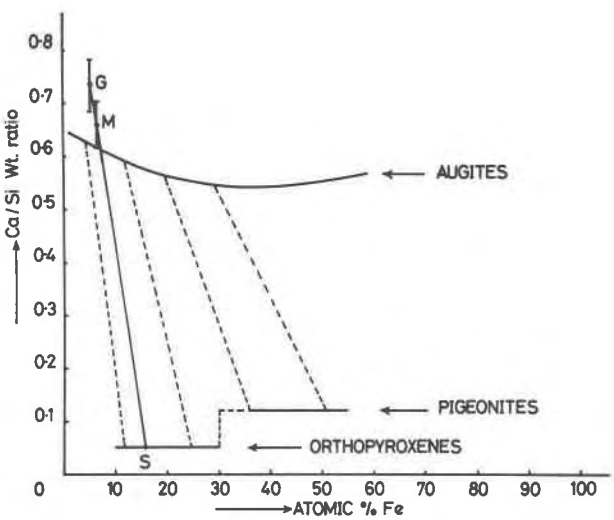

FIG. 5. Ca/Si weight ratio plotted as a function of atomic percent iron for coexisting pyroxenes in the Bushveld Complex. Some tie-lines are shown as dashed lines. The bulk composition of the Stillwater bronzite is shown at S and the calculated values for the exsolved clinopyroxene are shown plotted along a tie-line at G (for value obtained from glass standard) and M (from Mull pigeonite standard).

[3] The formation of a contamination ring rather than a contamination spot is not completely understood. The beam profile is approximately Gaussian, and the carbon may migrate across the surface from the hotter to cooler portion of the probe.

[4] The analyses of the Bushveld pyroxenes are, of course, bulk analyses of grains containing exsolxed Ca-poor phases and do not represent equilibrium compositions.

The Calcium Distribution Between the Augite Lamellae

During this investigation a series of analyses was carried out in the region between two of the augite lamellae. The position of the probe during the analysis can be seen from the contamination marks in Figure 6a; the observed ratios of the calcium and silicon characteristic X-ray intensities are plotted in Figure 6b. The readings have not been corrected for background, which was negligible; the error bars indicate the worst probable errors in the ratios, *i.e.*

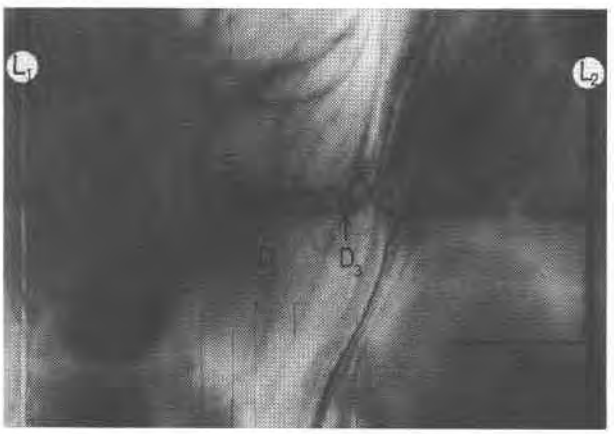

FIG. 6a. Electron micrograph showing two thick augite lamellae L_1 and L_2 with several thin (18 Å) lamellae and G.P. zones between them. The contamination spots mark the positions of the probe during analyses.

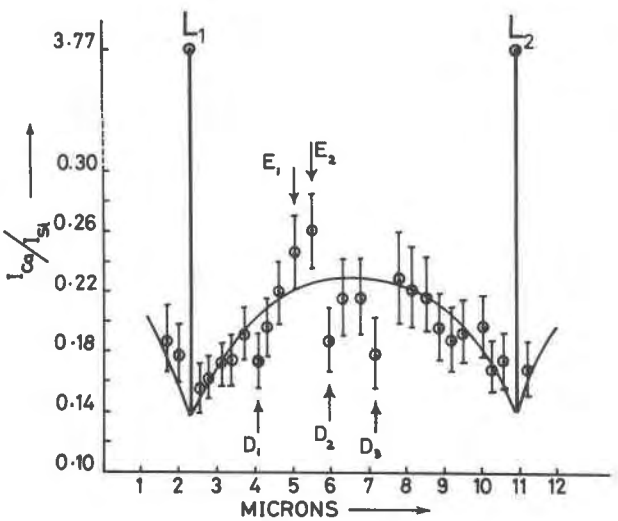

FIG. 6b. Graph showing the variation in calcium concentration from the area in Figure 6a. The positions marked E and D refer to areas enriched or depleted in calcium and correspond to thin lamellae and solute-depleted zones, respectively. L_1 and L_2 are the augite lamellae.

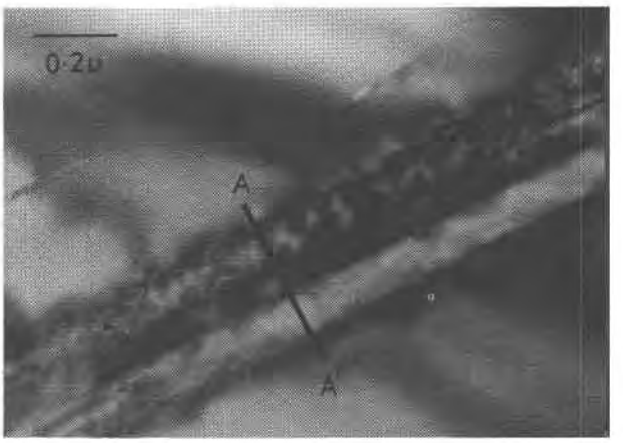

FIG. 7a. Electron micrograph of two large lamellae .075 apart.

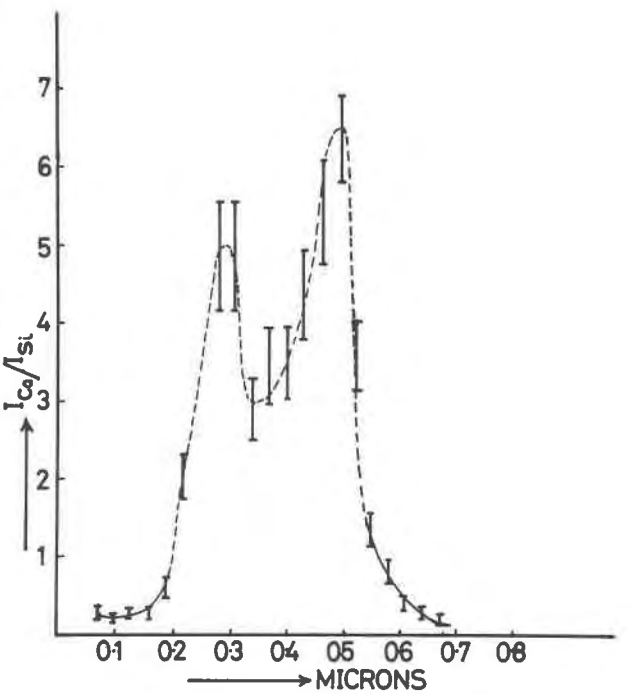

FIG. 7b. Graph showing the variation in calcium concentration across the lamellae in Figure 7a. The trace is along the line marked A-A′ above.

$$(N_{Ca}-\sigma_{Ca})/(N_{Si}+\sigma_{Si})$$

and

$$(N_{Ca}+\sigma_{Ca})/(N_{Si}-\sigma_{Si})$$

where N is the number of counts and $\sigma = \sqrt{N}$. The large error bars reflect the small number of counts, typically a few hundred. As can be seen from Figure 6b, there is a definite depletion of calcium in the matrix adjacent to the augite lamellae. This solute

depletion, which is consistent with the observed PFZ adjacent to the lamellae, is the diffusion profile produced during the growth of the augite (as discussed by Champness and Lorimer, 1972). The points which do not fall on the smooth curve in Figure 6b coincide with very thin lamellae, 18Å thick, which are responsible for the Ca/Si ratios above the curve, labelled E in Figure 6b, or the depleted zones associated with these thin lamellae which have produced Ca/Si ratios below the curve, labelled D in Figure 6b.

Figure 7a shows two augite lamellae which are approximately 0.1μ thick and 0.075μ apart; Figure 7b shows the Ca/Si trace obtained by carefully traversing the probe across them. Although the lamellae are incompletely resolved, a distinct 'dip' in the calcium concentration between the two lamellae has been detected. Both this result and that in Figure 6 provide interesting evaluations of the resolution and sensitivity, respectively, of EMMA-4. In Figure 6 the thin lamellae are 18Å thick and, assuming that they are augite of the composition given in Table 1 for the thick lamellae, the total amount of calcium within the area analyzed, a column of 0.2μ in diameter and approximately the same thickness, is 4×10^{-17} gms. In Figure 7 the spatial resolution for chemical analysis is less than $.075\mu$.

In summary, the unique combination of high resolution electron petrography, electron diffraction, and microprobe analysis available in EMMA-4 has proved that the instrument is a valuable ancillary tool for the characterization of the microstructure of minerals.

Acknowledgments

The authors would like to thank Professors R. B. Nicholson, E. Smith, and J. Zussman for providing laboratory facilities. We are extremely grateful to Professor G. M. Brown, Dr. P. Gay, and Dr. D. L. Hamilton for providing samples, to Mr. J. Bradley for sample preparation, and to Mr. G. Cliff for assisting in the operating of EMMA-4. EMMA-4 was purchased with a grant from S.R.C. and the ion-thinning machines were provided by N.E.R.C.

References

ATKINS, F. B. (1969) Pyroxenes of the Bushveld intrusion, South Africa. *J. Petrology*, **10**, 222–249.

BARBER, D. J. (1970) Thin foils of non-metals made for electron microscopy by sputter-etching. *J. Materials Sci.* 5, 1–8.

BOYD, F. R., AND G. M. BROWN (1969) Electron-probe study of pyroxene exsolution. *Mineral. Soc. Amer. Spec. Pap.* **2**, 211–216.

CHAMPNESS, P. E., AND G. W. LORIMER (1973) Precipitation (exsolution) in an orthopyroxene. *J. Materials Sci.* (in press).

———, AND G. W. LORIMER (1971) An electron microscopic study of a lunar pyroxene. *Contrib. Mineral. Petrology*, 33, 171–183.

CLIFF, G., AND G. W. LORIMER (1972) The quantitative analysis of thin metal foils using EMMA-4—the ratio technique. *Proc. Fifth European Congr. Electron Microscopy*. Institute of Physics, London, pp. 140–141.

COOKE, C. J., AND P. DUNCUMB (1968) Performance analysis of a combined electron microscope and micro-probe analyser EMMA. *5th. Int. Conf. X-ray Optics and Microanalysis, Tübingen*. Springer-Verlag, Berlin. pp. 245–247.

HALL, T. A. (1971) The microprobe assay of chemical elements. *In Physical Techniques in Biological Research*, 2nd edition, Vol. 1A, Ed. G. Oster. Academic Press, New York, pp. 157–275.

HALLIMOND, A. F. (1914) Optically uniaxial augite from Mull. *Mineral. Mag.* **17**, 97–99.

HENRY, N. F. M. (1942) Lamellar structure in orthopyroxenes. *Mineral Mag.* **26**, 179–189.

HESS, H. H. (1960) Stillwater igneous complex, Montana. *Geol. Soc. Amer. Mem.* **80**.

LORIMER, G. W., M. J. NASIR, R. B. NICHOLSON, K. NUTTALL, D. E. WARD, AND J. R. WEBB (1972) The use of an analytical electron microscope (EMMA-4) to investigate solute concentrations in thin metal foils. *Proc. Fifth Int. Mater. Symp.* California University Press, Berkeley, pp. 222–234.

Manuscript received, September 7, 1972; accepted for publication, November 29, 1972.